

## NIR spectroscopy of jarosites

Ray L. Frost\*, Rachael-Anne Wills, Wayde Martens and Matt Weier

Inorganic Materials Research Program, School of Physical and Chemical Sciences, Queensland University of Technology, GPO Box 2434, Brisbane Queensland 4001, Australia.

Published as:

Frost, Ray and Wills, Rachael-Anne and Weier, Matt and Martens, Wayde (2005) NIR spectroscopy of jarosites. *Spectrochimica Acta* 62(4-5):pp. 869-874.

Copyright Elsevier

### Abstract

Near-infrared spectroscopy (NIR) has been used to analyse a suite of synthesised jarosites of formula  $M_n(\text{Fe}^{3+})_6(\text{SO}_4)_4(\text{OH})_{12}$  where M is K, Na, Ag, Pb,  $\text{NH}_4^+$  and  $\text{H}_3\text{O}^+$ . Whilst the spectra of the jarosites show a common pattern differences in the spectra are observed which enable the minerals to be distinguished. The NIR bands in the 6300 to 7000  $\text{cm}^{-1}$  region are attributed to the first fundamental overtone of the infrared and Raman hydroxyl stretching vibrations. The NIR spectrum of the ammonium jarosite shows additional bands at 6460 and 6143  $\text{cm}^{-1}$  attributed to the first fundamental overtones of NH stretching vibrations. A set of bands are observed in the 4700 to 5500  $\text{cm}^{-1}$  region which are assigned to combination bands of the hydroxyl stretching and deformation vibrations. The ammonium jarosite shows additional bands at 4730 and 4621  $\text{cm}^{-1}$  attributed to the combination of NH stretching and bending vibrations. NIR spectroscopy has the ability to distinguish between the jarosite minerals even when the formula of the minerals is closely related. The NIR spectroscopic technique has great potential as a mineral exploratory tool on planets and in particular Mars.

**Keywords:** iron sulphates, natrojarosite, jarosite, plumbojarosite, argentojarosite, near-IR spectroscopy

### Introduction

Interest in the study of iron(II) sulphates arises from at least two perspectives. Firstly the observation of sulphates of iron on Mars by recent exploration and secondly by the formation of iron(II) and iron(III) sulphates in evaporate deposits [1]. Studies of these minerals have been undertaken for some considerable time [2-6].

Near IR spectroscopy provides a suitable method for the analysis of these types of materials [7-10]. The other use of near-IR spectroscopy is in the search for knowledge of minerals in the solar system [11-16]. Hunt et al. first applied NIR spectroscopy to the study of minerals [17, 18]. It should be recognised that Near-IR spectroscopy is known also as proton spectroscopy such that this type of spectroscopy

---

\* Author to whom correspondence should be addressed (r.frost@qut.edu.au)

is most useful for measuring bonds involving hydrogen such as OH, NH, CH etc. Thus the technique appears most suitable for the measurement of hydrated, hydroxylated sulphates as might be found in soils and sediments that may exist on Mars. The Mars mission rover known as opportunity has been used to discover the presence of jarosite on Mars, thus providing evidence for the existence or pre-existence of water on Mars.

(<http://www.news.cornell.edu/releases/rover/Mars.jarosite.html>)

Recent studies have identified iron sulphate minerals on Mars [19-22].

Thermal emission studies have been used to study minerals on Mars or at least to mimic possible models of Martian minerals [23-26]. Some studies attempt to model the possible equilibria of minerals such as the iron sulphates in an attempt to predict the geochemical evolution of Martian minerals [27]. This model proposes five stages of evolution of Martian minerals. The formation of iron(II) and iron(III) sulphates are included in this model. Such formation based upon chemical equilibria must include concentrated solutions and the effect of pH, temperature and other factors. Such equilibria are complex to say the least [28, 29]. One effective method of studying hydrated and hydroxylated minerals is to use NIR spectroscopy. The existence of iron(II) and iron(III) sulphate minerals would confirm the existence/pre-existence of water on Mars. The advantages of NIR spectroscopy include remote sensing, sensitivity to minerals containing OH and NH groups and the ease of operation of the technique.

In order to determine the presence of specific minerals on planets such as Mars or the moons of Saturn using NIR spectroscopy, it is necessary to build a data base of NIR spectra of minerals. Recent exploration of Mars has indicated using Mossbauer Spectroscopy the presence of iron minerals such as hematite which has formed in small nodules. Such secondary minerals can be formed from solution. This of course is an indication of the pre-existence of water on Mars. Not only should the data base contain natural minerals i.e. earth stable structures but also unstable structures since both the physical and chemical conditions on planets may be very different to the conditions on earth. The technique of NIR spectroscopy is very relevant to the study of minerals on planets such as Mars since the miniaturisation of the technology is possible. In this research we report the NIR spectroscopy of synthetic jarosites.

## **Experimental**

### ***Minerals***

The jarosite minerals of formula  $M_n(Fe^{3+})_6(SO_4)_4(OH)_{12}$  where M is K, Na, Ag, Pb,  $NH_4^+$  and  $H_3O^+$  were synthesised. The minerals were analysed by X-ray diffraction for phase identification and the minerals have been analysed by electron microprobe analysis for composition.

### **Near-infrared spectroscopy (NIR)**

Near IR spectra were collected on a Nicolet Nexus FT-IR spectrometer with a

Nicolet Near-IR Fibreport accessory. A white light source was used, with a quartz beam splitter and TEC NIR InGaAs detector. Spectra were obtained from 11 000 to 4000  $\text{cm}^{-1}$  by the co-addition of 64 scans at a resolution of  $8\text{cm}^{-1}$ . A mirror velocity of 1.266 m/sec was used. The spectra were transformed using the Kubelka-Munk algorithm to provide spectra for comparison with absorption spectra. Infrared absorption spectra were obtained using the KBr pressed pellet technique using a Perkin-Elmer FT-IR spectrometer 2000 bench using  $4\text{ cm}^{-1}$  resolution with 128 scans. Infrared spectra were obtained using a Nicolet Nexus 870 FTIR spectrometer with a smart endurance single bounce diamond ATR cell. Spectra over the 4000–525  $\text{cm}^{-1}$  range were obtained by the co-addition of 64 scans with a resolution of  $4\text{ cm}^{-1}$  and a mirror velocity of 0.6329 cm/s. Spectra were co-added to improve the signal to noise ratio.

Spectral manipulation such as baseline adjustment, smoothing and normalisation were performed using the Spectralcalc software package GRAMS (Galactic Industries Corporation, NH, USA). Band component analysis was undertaken using the Jandel 'Peakfit' software package which enabled the type of fitting function to be selected and allows specific parameters to be fixed or varied accordingly. Band fitting was done using a Lorentz-Gauss cross-product function with the minimum number of component bands used for the fitting process. The Gauss-Lorentz ratio was maintained at values greater than 0.7 and fitting was undertaken until reproducible results were obtained with squared correlations of  $r^2$  greater than 0.995.

## Results and discussion

Interest in jarosites results from their discovery on the planet Mars. The Near-IR spectral regions of jarosites may be conveniently divided into four regions (a) the high wavenumber region  $> 7500\text{ cm}^{-1}$  (b) the high wavenumber region between 6400 and  $7400\text{ cm}^{-1}$  attributed to the first overtone of the fundamental hydroxyl stretching mode (c) the  $5500\text{-}6300\text{ cm}^{-1}$  region attributed to water combination modes of the hydroxyl fundamentals of water, and (d) the  $4000\text{-}5500\text{ cm}^{-1}$  region attributed to the combination of the stretching and deformation modes of jarosites. The NIR spectra of the jarosites in the high wavenumber region are shown in [Figure 1](#). The results of the analysis of the spectra are reported in [Table 1](#). The spectra of the OH stretching region of the synthetic jarosites are shown in [Figure 2](#). The results of the spectral analysis are reported in [Table 2](#).

The spectra in [Figure 1](#) clearly show that the peak maximum is observed at different positions for the different jarosites. The peak is at 6844 (K-jarosite), 6798 (Na-jarosite), 6808 (Pb-jarosite), 6777 (Ag-jarosite) 6865 ( $\text{NH}_4$ -jarosite) and 6829  $\text{cm}^{-1}$  (hydronium jarosite). The spectral profile can be curve resolved into the component bands as is illustrated in [Figure 1](#). Three component bands are observed for K-jarosite at 7004, 6822 and  $6677\text{ cm}^{-1}$ . These bands which are the first fundamental overtone of the hydroxyl stretching vibrations are the result of the doubling of the wavenumbers of the OH stretching vibrations. For K-jarosite three infrared OH stretching bands are found at 3375.9, 3317.9 and  $3094.3\text{ cm}^{-1}$ . It must be remembered that these overtones can be the doubling of Raman bands as well as the infrared bands will be NIR active. For K-jarosite two Raman bands are found at 3434 and  $3392\text{ cm}^{-1}$ . It is possible that the infrared and Raman hydroxyl vibrations can combine to give the hydroxyl overtones. The band at  $6677.4\text{ cm}^{-1}$  is the most intense

band (12.2 %) (refer Table 1). This band is likely to arise from the doubling of the  $3375.9\text{ cm}^{-1}$  band. The band at  $6822\text{ cm}^{-1}$  (6.8%) may arise from the doubling of the Raman  $3434\text{ cm}^{-1}$  band.

For Na jarosite, two major NIR bands are observed at  $6681.8$  and  $6789.9\text{ cm}^{-1}$  with two other bands at  $6378$  and  $6976\text{ cm}^{-1}$ . The relative intensities of these NIR bands are 15.4, 8.8, 8.2 and 1.6 %. Three mid-IR bands are observed at  $3354$ ,  $3321$ ,  $3181\text{ cm}^{-1}$  with relative intensities of 2.4, 6.0 and 9.0%. For Na-jarosites three Raman bands are observed at  $3438$ ,  $3410$  and  $3385\text{ cm}^{-1}$ . Thus it is possible that the  $6681.8\text{ cm}^{-1}$  band is the first fundamental overtone of the mid-IR band at  $3354\text{ cm}^{-1}$  and the band at  $6789\text{ cm}^{-1}$  is the combination of the infrared band at  $3354$  and the Raman band at  $3438\text{ cm}^{-1}$ . The band at  $6378\text{ cm}^{-1}$  is the first overtone of the mid-IR band at  $3181\text{ cm}^{-1}$ . In the case of lead jarosite, two intense NIR bands are observed at  $6809.7$  and  $6552.8\text{ cm}^{-1}$  with relative intensities of 15 % each. Two mid-IR bands are observed at  $3326.0$  and  $3163.5\text{ cm}^{-1}$  and a broad intense Raman band is observed at  $3410\text{ cm}^{-1}$ . It is apparent that the band at  $6809\text{ cm}^{-1}$  is the first fundamental overtone of the Raman band at  $3410\text{ cm}^{-1}$  and the band at  $6552.8\text{ cm}^{-1}$  may be the first fundamental overtone of the mid-IR band at  $3326\text{ cm}^{-1}$ .

For Ag-jarosite, the NIR pattern is similar to that of Na-jarosite. Two intense NIR bands are observed for Ag-jarosite at  $6769.8$  and  $6548.4\text{ cm}^{-1}$ . In the mid-IR spectrum, three intense bands are observed at  $3344.7$ ,  $3257.6$  and  $3012.1\text{ cm}^{-1}$ . Three Raman bands are also observed for the Ag-jarosite at  $3449$ ,  $3401$  and  $3375\text{ cm}^{-1}$ . One probable assignment of the NIR bands is that the bands at  $6769.8$  and  $6548.4\text{ cm}^{-1}$  are the first fundamental overtones of the Raman band at  $3449$  and the infrared band at  $3344.7\text{ cm}^{-1}$ .

The hydronium jarosite NIR spectrum is a less complex spectrum than the previous examples. The spectrum is composed of two overlapping bands at  $6815$  and  $6634\text{ cm}^{-1}$  with relative intensities of 16.9 and 18.5 %. The mid-IR spectrum of hydronium jarosite also shows two mid-IR bands at  $3358.7$  and  $3219.1\text{ cm}^{-1}$ . The Raman spectrum of the hydronium jarosite shows an intense band at  $3415\text{ cm}^{-1}$  with a shoulder at  $3388\text{ cm}^{-1}$ . The conclusion is reached that the two NIR bands at  $6815$  and  $6634\text{ cm}^{-1}$  are the first fundamental overtones of the Raman band at  $3415$  and the infrared band at  $3358.7\text{ cm}^{-1}$ . The conclusion is made that the NIR spectrum of jarosites is fundamentally composed of the first fundamental overtones of the Raman and infrared hydroxyl stretching vibrations. The case of the ammonium jarosite is significantly more complex since the NIR spectrum contains the first fundamental overtones not only of the OH but also the NH vibrations. The NIR spectrum of ammonium jarosite consists of a suite of bands at  $6985$ ,  $6859$ ,  $6719$ ,  $6460$  and  $6143\text{ cm}^{-1}$  with relative intensities of 1.9, 2.2, 7.6, 7.6 and 1.6 %. The mid-IR spectrum of ammonium jarosite shows four bands at  $3407$ ,  $3316.5$ ,  $3212.2$  and  $3062.2\text{ cm}^{-1}$  with relative intensities of 5.1, 2.7, 5.7 and 1.4 %. The first two bands are attributed to OH stretching vibrations and the latter two to NH stretching vibrations. The NIR spectrum of the ammonium jarosite is too complex to make any realistic attempt to assign the bands. It is not known whether NH and OH bands would combine to give bands in the NIR spectrum. This seems unlikely.

The NIR spectra in the  $4000$  to  $5500\text{ cm}^{-1}$  region of jarosites are shown in **Figure 3**. This region may be divided into two sections (a)  $4000$  to  $4700\text{ cm}^{-1}$  and (b)  $4700$  to  $5500\text{ cm}^{-1}$ . In all of the spectra there is a common band which is of low

intensity at around  $5405\text{ cm}^{-1}$  (K-jarosite  $5405.5$ , Na-jarosite  $5413$ , Pb-jarosite  $5435.9$ , Ag-jarosite  $3409.6$  hydronium jarosite  $5430\text{ cm}^{-1}$ ). This band is ascribed to adsorbed water. The hydronium jarosite shows a strong band at  $5073\text{ cm}^{-1}$ . This band is also present in the ammonium jarosite and is observed as two bands at  $5196$  and  $5114\text{ cm}^{-1}$ . There are bands in similar positions for the other jarosites (K- $5205$  and  $5116$ ; Na- $5178$  and  $5101$ ; Pb- $5163$  and  $5095$ ; Ag- $5172$  and  $5108\text{ cm}^{-1}$ ). In the infrared spectrum of jarosites such as the hydronium jarosite an intense band is observed at around  $980\text{ cm}^{-1}$  and is not observed in the Raman spectrum. This band is assigned to the hydroxyl deformation mode in jarosites. It is possible that the band at  $5073\text{ cm}^{-1}$  for the hydronium jarosite is a combination of the hydroxyl stretching and hydroxyl deformation modes. For the ammonium jarosite additional bands are observed at  $4917$ ,  $4730$ ,  $4621$  and  $4418\text{ cm}^{-1}$ . These bands must be due to the combination of NH stretching and bending modes. For hydronium jarosite a band is observed at  $4438\text{ cm}^{-1}$  which is also observed for the ammonium jarosite at  $4418\text{ cm}^{-1}$ . The band is a common band in jarosites (K- $4420$ ; Na- $4419$ ; Pb- $4445$ ; Ag- $4396\text{ cm}^{-1}$ ). The band shows more complexity for the Pb-jarosite.

## Conclusions

Near-IR spectroscopy is a technique, which has not been previously applied in depth to the study of jarosites. Indeed jarosites by their very nature, being composed of adsorbed water and hydroxyl units coordinated to Fe(III) ion, lend themselves to study by NIR. NIR reflectance techniques have proven most useful for the analysis of jarosites. As such the technique could be applicable to the study of these types of minerals by remote sensing or by a stand-off spectroscopic technique. NIR spectroscopy has the ability to distinguish between the jarosite minerals even when the formula of the minerals is closely related. The NIR spectroscopic technique has great potential as a mineral exploratory tool on planets and in particular Mars.

## Acknowledgments

The financial and infra-structure support of the Queensland University of Technology Inorganic Materials Research Program of the School of Physical and Chemical Sciences is gratefully acknowledged. The Australian Research Council (ARC) is thanked for funding.

## References

- [1]. T. Buckby, S. Black, M. L. Coleman and M. E. Hodson, *Min. Mag.* 67 (2003) 263.
- [2]. F. Cesbron, *Bull. Soc. Franc. Mineral. Crist.* 87 (1964) 125.
- [3]. W. H. Baur, *Fortschritte der Mineralogie* 39 (1961) 333.
- [4]. E. G. Ehlers and D. V. Stiles, *Am. Min.* 50 (1965) 1457.
- [5]. R. Scharizer, *Zeitschrift fuer Kristallographie und Mineralogie* 43 (1907) 113.
- [6]. R. Scharizer, *Zeitschrift fuer Kristallographie und Mineralogie* 46 (1909) 427.
- [7]. M. Long and S.-Q. Pei, *Yankuang Ceshi* 22 (2003) 169.
- [8]. C. A. Russell, *Comm. Soil Sc. Plant Anal.* 34 (2003) 1557.
- [9]. J. W. Van Groenigen, C. S. Mutters, W. R. Horwath and C. Van Kessel, *Plant and Soil* 250 (2003) 155.
- [10]. C.-W. Chang, D. A. Laird, M. J. Mausbach and C. R. Hurburgh, Jr., *Soil Sc. Soc. Amer. Journal* 65 (2001) 480.
- [11]. I. Biering, K. Larsen, T. Garp, D. H. Christensen, C. B. Koch, P. W. Jensen and O. F. Nielsen, *Asian Chem. Letts* 7 (2003) 99.
- [12]. T. H. Burbine and R. P. Binzel, *Icarus* 159 (2002) 468.
- [13]. C. D. Cooper and J. F. Mustard, *Icarus* 158 (2002) 42.
- [14]. N. Hirao, *Ganseki Kobutsu Kagaku* 31 (2002) 111.
- [15]. L. A. Mcfadden, D. D. Wellnitz, M. Schnaubelt, M. J. Gaffey, J. F. Bell, Iii, N. Izenberg, S. Murchie and C. R. Chapman, *Meteoritics & Planetary Science* 36 (2001) 1711.
- [16]. G. Bellucci, *Earth, Moon, and Planets* 78 (1999) 305.
- [17]. G. R. Hunt and R. C. Evarts, *Geophysics* 46 (1981) 316.
- [18]. G. R. Hunt and R. P. Ashley, *Economic Geology and the Bulletin of the Society of Economic Geologists* 74 (1979) 1613.
- [19]. J.-P. Bibring, Y. Langevin, F. Poulet, A. Gendrin, B. Gondet, M. Berthe, A. Soufflot, P. Drossart, M. Combes, G. Bellucci, V. Moroz, N. Mangold and B. Schmitt, *Nature* 428 (2004) 627.
- [20]. M. E. Elwood Madden, R. J. Bodnar and J. D. Rimstidt, *Nature* 431 (2004) 821.
- [21]. M. E. E. Madden, R. J. Bodnar and J. D. Rimstidt, *Nature* 431 (2004) 821.
- [22]. D. T. Vaniman, D. L. Bish, S. J. Chipera, C. I. Fialips, J. William Carey and W. C. Feldman, *Nature* 431 (2004) 663.
- [23]. J. R. Michalski, M. D. Kraft, T. Diedrich, T. G. Sharp and P. R. Christensen, *Geophysical Res. Letts* 30 (2003) PLA2/1.
- [24]. D. L. Bish, J. William Carey, D. T. Vaniman and S. J. Chipera, *Icarus* 164 (2003) 96.
- [25]. M. D. Lane and P. R. Christensen, *Icarus* 135 (1998) 528.
- [26]. R. L. Huguenin, *J. Geophys. Res.* 79 (1974) 3895.
- [27]. G. M. Marion, D. C. Catling and J. S. Kargel, *Geochimica et Cosmochimica Acta* 67 (2003) 4251.
- [28]. F. K. Cameron, *J. Phys. Chem.* 34 (1930) 692.
- [29]. E. Posnjak and H. E. Merwin, *J. Am. Chem. Soc.* 44 (1922) 1965.

Potassium Jarosite			Sodium Jarosite			Lead Jarosite			Silver Jarosite			Ammonium Jarosite			Hydronium Jarosite		
Centr e	FWH M	% Area	Centr e	FWH M	% Area	Centr e	FWH M	% Area	Centr e	FWH M	% Area	Centr e	FWH M	% Area	Centr e	FWH M	% Area
<b>7004.6</b>	208.8	5.2															
			<b>6976.9</b>	114.4	1.6				<b>6961.0</b>	145.6	2.4	<b>6985.8</b>	184.2	1.9			
												<b>6859.2</b>	136.2	2.2			
<b>6822.1</b>	231.3	6.8				<b>6809.7</b>	281.6	15.0							<b>6815.1</b>	205.1	16.9
			<b>6789.9</b>	154.6	8.8	<b>6790.9</b>	170.5	4.0									
									<b>6769.8</b>	209.4	12.2	<b>6719.2</b>	291.7	7.6			
<b>6677.4</b>	450.4	12.2	<b>6681.8</b>	351.0	15.4												
						<b>6552.8</b>	355.8	15.0	<b>6548.4</b>	504.5	19.1				<b>6634.1</b>	386.1	18.5
												<b>6460.5</b>	290.8	7.6			
			<b>6378.4</b>	439.4	8.2				<b>6271.1</b>	293.8	3.5						
									<b>6139.9</b>	310.9	2.6	<b>6143.0</b>	269.1	1.6			
			<b>5498.2</b>	75.8	0.7	<b>5435.9</b>	67.1	3.3							<b>5430.4</b>	58.3	1.3
<b>5405.5</b>	51.1	0.5	<b>5413.2</b>	79.9	5.2				<b>5409.6</b>	78.5	2.5				<b>5412.2</b>	86.8	2.0
												<b>5396.2</b>	60.6	0.7			
						<b>5366.0</b>	78.9	1.5	<b>5376.9</b>	60.6	1.3						
						<b>5315.7</b>	46.2	0.5									
			<b>5238.5</b>	49.1	0.8				<b>5237.9</b>	58.0	1.3						
<b>5205.9</b>	116.8	14.2										<b>5196.0</b>	104.3	3.6			
			<b>5178.1</b>	78.0	5.5				<b>5172.3</b>	70.8	4.2						
						<b>5163.8</b>	82.3	3.2									
<b>5116.6</b>	162.3	20.8										<b>5114.3</b>	143.7	7.0			
			<b>5101.3</b>	131.3	10.2				<b>5108.7</b>	139.0	11.8						

						<b>5094.9</b>	109.4	3.7							<b>5084.7</b>	44.6	0.4
															<b>5073.3</b>	181.4	18.8
<b>4978.2</b>	217.6	19.8	<b>4993.9</b>	193.6	18.3	<b>4996.2</b>	153.2	7.2	<b>4990.3</b>	207.2	17.4	<b>4983.9</b>	82.4	2.6			
												<b>4917.7</b>	247.7	27.7	<b>4920.5</b>	186.1	3.7
						<b>4872.7</b>	138.0	3.7									
<b>4811.8</b>	128.5	2.9	<b>4837.4</b>	149.9	6.7				<b>4826.9</b>	138.0	3.7						
												<b>4730.4</b>	130.5	6.6			
												<b>4621.2</b>	249.9	11.2			
															<b>4532.3</b>	133.9	7.2
<b>4512.8</b>	119.2	4.4				<b>4507.7</b>	136.7	8.5									
			<b>4496.4</b>	138.1	4.2												
						<b>4445.6</b>	69.5	10.5		<b>4478.8</b>	150.7	5.4					
<b>4420.4</b>	68.5	4.6	<b>4419.3</b>	36.0	1.2							<b>4418.4</b>	86.2	3.8	<b>4438.2</b>	88.0	16.6
			<b>4408.3</b>	96.9	7.5												
<b>4384.4</b>	45.7	0.9							<b>4396.3</b>	88.0	11.3						
						<b>4371.2</b>	81.2	10.8							<b>4374.0</b>	84.9	6.8
<b>4355.7</b>	29.7	0.3															
						<b>4316.8</b>	46.1	1.1									
						<b>4153.1</b>	71.5	4.5									
			<b>4127.2</b>	100.7	4.7												
<b>4111.9</b>	134.8	5.0															
						<b>4102.9</b>	58.1	2.7	<b>4100.7</b>	111.5	4.9						
			<b>4068.4</b>	22.2	1.0										<b>4070.7</b>	173.2	7.5
<b>4051.9</b>	58.3	2.3															
<b>3999.7</b>	312.7	0.0	<b>3999.7</b>	170.0	0.0	<b>3991.9</b>	177.0	1.3	<b>3999.7</b>	263.9	0.0				<b>4000.8</b>	58.7	0.3
												<b>3907.4</b>	0.0	16.0			

**Table 1 Analysis of the NIR spectra of jarosites of K, Na, Ag, Pb, NH<sub>4</sub><sup>+</sup> and H<sub>3</sub>O<sup>+</sup>**

Potassium Jarosite			Sodium Jarosite			Lead Jarosite			Silver Jarosite			Ammonium Jarosite			Hydronium Jarosite		
Centre	FWHM	% Area	Centre	FWHM	% Area	Centre	FWHM	% Area	Centre	FWHM	% Area	Centre	FWHM	% Area	Centre	FWHM	% Area
															<b>3469.6</b>	65.2	0.3
						<b>3447.6</b>	83.4	0.7									
												<b>3407.1</b>	94.3	5.1			
<b>3375.9</b>	94.5	1.7															
			<b>3354.4</b>	60.7	2.4												
						<b>3345.0</b>	41.1	0.5	<b>3344.7</b>	135.2	6.4						
<b>3317.9</b>	324.5	12.7	<b>3321.5</b>	162.9	6.0	<b>3326.0</b>	182.9	9.5				<b>3316.5</b>	103.4	2.7			
												<b>3257.6</b>	288.6	9.9			
															<b>3212.2</b>	162.0	5.7
			<b>3181.1</b>	276.6	9.0										<b>3219.1</b>	283.7	7.7
						<b>3163.5</b>	175.6	2.6									
<b>3094.3</b>	445.7	8.5															
												<b>3062.2</b>	128.9	1.4			
									<b>3012.1</b>	300.3	3.6						
															<b>2362.7</b>	17.8	0.1
															<b>2332.3</b>	30.0	0.1
															<b>2073.8</b>	91.6	0.4
			<b>2053.7</b>	80.4	0.4												
						<b>2025.7</b>	150.4	0.6	<b>2035.0</b>	146.8	0.7						
															<b>2003.8</b>	94.9	0.3
			<b>1987.2</b>	36.2	0.2												
			<b>1642.2</b>	65.7	0.4										<b>1670.6</b>	117.5	1.0
															<b>1637.6</b>	55.0	0.6
<b>1632.4</b>	79.7	1.0				<b>1625.1</b>	124.1	0.9	<b>1622.5</b>	112.5	1.3	<b>1631.5</b>	85.1	0.6			

**Table 2** Results of the spectral analysis of the OH stretching region of jarosites.

### **List of Figures**

Figure 1 NIR spectra in the first OH fundamental overtone of jarosites in the 5800 to 7350  $\text{cm}^{-1}$  range.

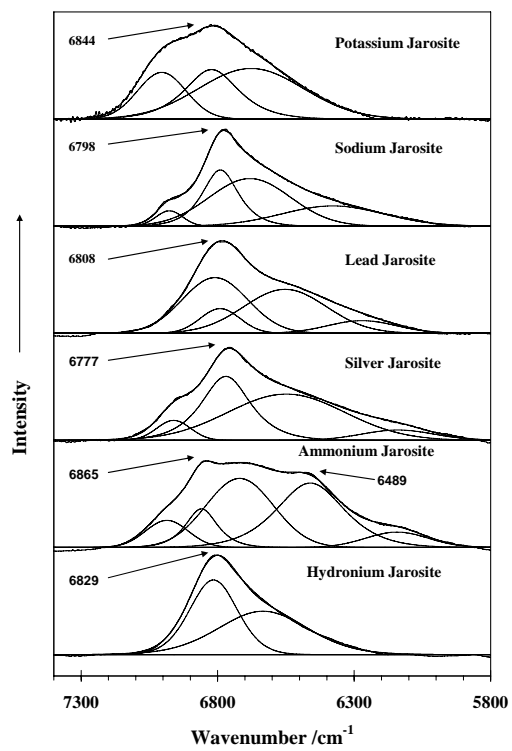
Figure 2 Mid-IR spectra of the OH stretching region in the 2600 to 3800  $\text{cm}^{-1}$  range.

Figure 3 NIR spectra of jarosites in the 4000 to 5550  $\text{cm}^{-1}$  range.

### **List of Tables**

**Table 1 Analysis of the NIR spectra of jarosites of K, Na, Ag, Pb,  $\text{NH}_4^+$  and  $\text{H}_3\text{O}^+$**

**Table 2 Results of the spectral analysis of the OH stretching region of jarosites.**



**Figure 1**

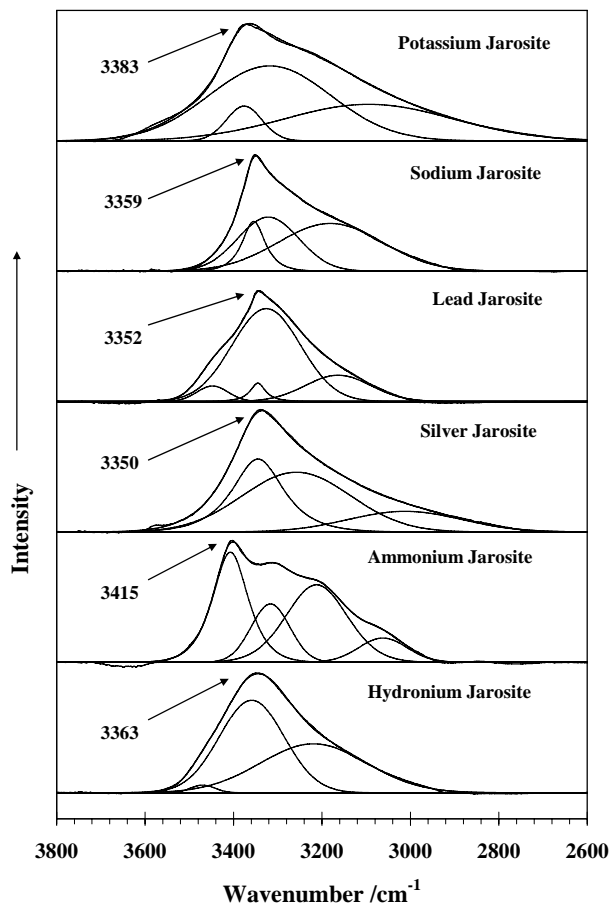


**Figure 2**

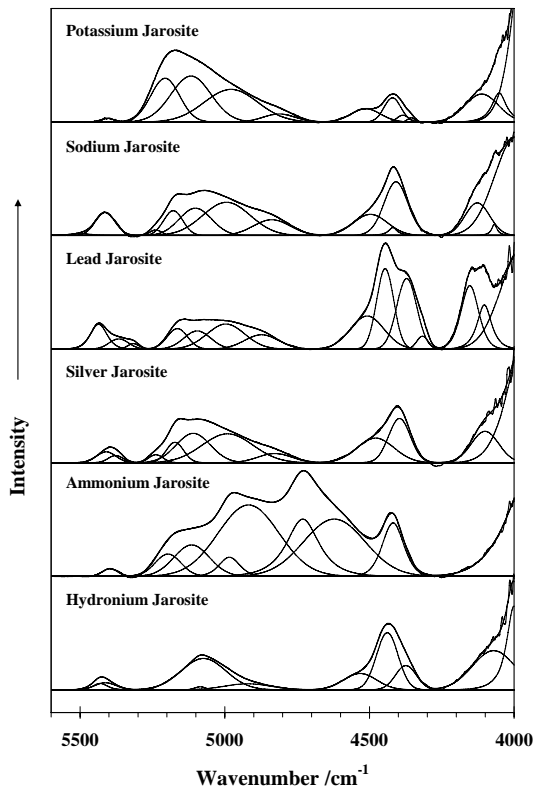


**Figure 3**

